**Biogeosciences
Discussions**

Groundwater and porewater as a major source of alkalinity to a fringing coral reef lagoon (Muri Lagoon, Cook Islands)

T. Cyronak, I. R. Santos, D. V. Erler, and B. D. Eyre

Centre for Coastal Biogeochemistry, School of Environment, Science and Engineering, Southern Cross University, Lismore, New South Wales, Australia

Correspondence to: T. Cyronak (tcyronak@gmail.com)

Discussion Paper | Discussion Paper | Discussion Paper | Discussion Paper

BGD

9, 15501–15540, 2012

Groundwater and porewater as a major source of alkalinity

T. Cyronak et al.

Title Page

Abstract	Introduction
Conclusions	References
Tables	Figures

|◄ | ►|

◄ | ►

Back | Close

Full Screen / Esc

Printer-friendly Version

Interactive Discussion

Full Screen / Esc

Printer-friendly Version

Interactive Discussion

Abstract

To better predict how ocean acidification will affect coral reefs, it is important to understand how biogeochemical cycles on reefs alter carbonate chemistry over various temporal and spatial scales. This study quantifies the contribution of fresh groundwater discharge (as traced by radon) and shallow porewater exchange (as quantified from advective chamber incubations) to total alkalinity (TA) dynamics on a fringing coral reef lagoon along the southern Pacific island of Rarotonga over a tidal and diel cycle. Benthic alkalinity fluxes were affected by the advective circulation of water through permeable sediments, with net daily flux rates of carbonate alkalinity ranging from -1.55 to $7.76\,\text{mmol m}^{-2}\,\text{d}^{-1}$, depending on the advection rate. Submarine groundwater discharge (SGD) was a source of TA to the lagoon, with the highest flux rates measured at low tide, and an average daily TA flux of $1080\,\text{mmol m}^{-2}\,\text{d}^{-1}$. Both sources of TA were important on a reef wide basis, although SGD acted solely as a delivery mechanism of TA to the lagoon, while porewater advection was either a sink or source of TA dependant on the time of day. On a daily basis, groundwater can contribute approximately 70 % to 80 % of the TA taken up by corals within the lagoon. This study describes overlooked sources of TA to coral reef ecosystems that can potentially alter water-column carbonate chemistry. We suggest that porewater and groundwater fluxes of TA should be taken into account in ocean acidification models in order to properly address changing carbonate chemistry within coral reef ecosystems.

1 Introduction

The recent increase in atmospheric CO_2 has led to an increase in oceanic $p\text{CO}_2$ as roughly 30 % of anthropogenic CO_2 has been absorbed by the oceans (Feely et al., 2004; Sabine et al., 2004; Orr et al., 2005; Doney et al., 2009). Ocean acidification is the term given to this increase in oceanic $p\text{CO}_2$, which alters the carbonate chemistry of seawater leading to a reduction in pH at a rate of roughly $0.002\,\text{pH y}^{-1}$ (Feely et

Groundwater and porewater as a major source of alkalinity

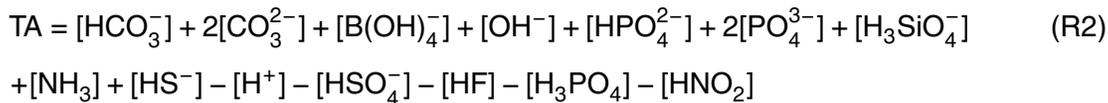T. Cyronak et al.

al., 2004; Doney et al., 2009). Ocean acidification can have drastic effects on biological processes and the biogeochemistry of marine ecosystems, with coral reefs being some of the most susceptible ecosystems (Fabry et al., 2008; De'ath et al., 2009). The biogeochemical processes occurring on coral reefs can modify the carbonate chemistry of the overlying seawater, leading to large diel variations in alkalinity, $p\mathrm{CO_2}$, pH, and dissolved oxygen (DO) (Santos et al., 2011; Shamberger et al., 2011; Gray et al., 2012; Shaw et al., 2012). In order to understand how ocean acidification will affect coral reefs, it is important to understand how natural processes, which can potentially buffer or intensify changes in $p\mathrm{CO_2}$, alter the carbonate chemistry of seawater within coral reef ecosystems.

As $\mathrm{CO_2}$ dissolves in water it is hydrolyzed to form carbonic acid in the following equilibrium reactions:

$$\mathrm{CO_2 + H_2O \leftrightarrow H_2CO_3 \leftrightarrow H^+ + HCO_3^- \leftrightarrow 2H^+ + CO_3^{2-}} \tag{R1}$$
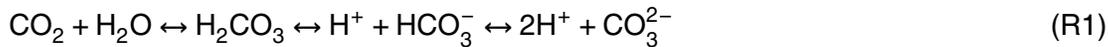
Due to the production of $\mathrm{HCO_3^-}$ and $\mathrm{CO_3^{-2}}$, the increase in $\mathrm{H^+}$ ions causes a reduction in seawater pH but does not change the total alkalinity (TA) (Millero, 1979; Zeebe and Wolf-Gladrow, 2001). The TA of a solution represents the ability of the solution to absorb $\mathrm{H^+}$ ions without an associated reduction in the pH, and in seawater is equal to the following equation (Wolf-Gladrow et al., 2007):

$$\mathrm{TA = [HCO_3^-] + 2[CO_3^{2-}] + [B(OH)_4^-] + [OH^-] + [HPO_4^{2-}] + 2[PO_4^{3-}] + [H_3SiO_4^-]} \tag{R2}$$

$$\mathrm{+ [NH_3] + [HS^-] - [H^+] - [HSO_4^-] - [HF] - [H_3PO_4] - [HNO_2]}$$

Within the range of normal oceanic pH, and especially in oligotrophic waters, the majority of alkalinity in seawater is found in the form of dissolved inorganic carbon (DIC) as $\mathrm{HCO_3^-}$ and $\mathrm{CO_3^{-2}}$ (Millero, 1979; Wolf-Gladrow et al., 2007).

The dissolution and precipitation of carbonate minerals, both biotic and abiotic, can alter the water-column TA within coral reef lagoons (Andersson et al., 2007; Rao et al., 2012). These changes in TA are large enough that ecosystem calcification rates have historically been measured using the alkalinity anomaly technique (Chisholm and

Gattuso, 1991; Gattuso et al., 1996), which relies on the measuring the change in water-column TA according to the following equation:

$$CaCO_3 \leftrightarrow Ca^{2+} + CO_3^{2-} \tag{R3}$$

TA measurements are widely used in ocean acidification research to quantify community calcification rates (Shamberger et al., 2011; Silverman et al., 2012), measure sediment precipitation and dissolution rates (Andersson et al., 2007; Cyronak et al., 2013), correct net ecosystem production calculations for inorganic carbon contributions (Frankignoulle et al., 1996; Gattuso et al., 1996; Suzuki and Kawahata, 2003), and to measure reef dissolution and bioerosion (Lazar and Loya, 1991; Zundelevich et al., 2007; Manzello et al., 2008). Also, it has been suggested that alkalinity generated from sediment dissolution may act as a partial buffer against any decrease in pH associated with ocean acidification, (Kleypas and Langdon, 2006; Morse et al., 2006), although this buffering capacity is still being debated (see Andersson and Mackenzie, 2012). The widespread use of TA in ocean acidification research makes it important to constrain all sources and sinks of TA within coral reef ecosystems.

The exchange of solutes between the water-column and permeable carbonate sediments is driven mainly by advective processes (Precht and Huettel, 2003; Santos et al., 2012). Porewater advection can occur on various temporal and spatial scales resulting in numerous exchange rates over variable time scales (Santos et al., 2012). Flow and topography induced pore water exchange (see Fig. 1(5) in Santos et al., 2012) is probably the dominant process driving porewater exchange within coral reef lagoons due to the formation of ripples and crests within permeable carbonate sediments (Precht and Huettel, 2003). These processes act on short temporal (min to h) and small spatial scales (cm) to induce the exchange of porewater solutes with the overlying water-column (Precht and Huettel, 2003). Porewater advection has a stimulatory effect on biological processes occurring within the sediments (Cook and Røy, 2006; Eyre et al., 2008; Glud et al., 2008) and has also been shown to have a stimulatory effect on TA fluxes, with increasing advection rates increasing net daily TA fluxes (Rao et al., 2012; Cyronak et al., 2013). However, while coral reef community calcification rates

are negatively correlated with the aragonite saturation state (Ω_{Ar}) of the water-column (see Fig. 6 in Shamberger et al., 2011), carbon cycling in permeable sediments cannot be easily predicted by Ω_{Ar} of the overlying water-column (Cyronak et al., 2013).

Submarine groundwater discharge (SGD) has been shown to be in an important component of freshwater delivery to coastal ecosystems, on the scale of 6 % to 10 % of surface water flow, which amounts to an estimated $10\,000\,\mathrm{l\,m^{-1}\,d^{-1}}$ along the global coast (Burnett et al., 2003; Santos et al., 2012). The few studies assessing SGD rates on coral reefs describe a range from 52 to $4732\,\mathrm{l\,m^{-1}\,h^{-1}}$, and suggest that SGD can be an important source of solutes to coral reef ecosystems (Lewis, 1987; D'Elia and Wiebe, 1990; Paytan et al., 2006). There are multiple methods to estimate SGD into coastal ecosystems including seepage meters, piezometers, natural tracers, water balance approaches, and theoretical modeling (Burnett et al., 2006). Due to its naturally high concentrations in groundwater compared to surface waters, and its unreactive nature, ^{222}Rn has been used as a natural tracer for groundwater in aquatic systems for decades (Cable et al., 1996; Burnett et al., 2006). Mass balance models using ^{222}Rn have been developed that estimate SGD fluxes into coastal ecosystems (Burnett and Dulaiova, 2003).

Groundwater concentrations of TA can be higher than oceanic waters and encompasses a broad range from 90 to $23\,300\,\mathrm{\mu mol\,l^{-1}}$ (Mahlknecht et al., 2004; Rad et al., 2007; Moore et al., 2011; Schopka and Derry, 2012). Using radium based SGD efflux rates, Moore et al. (2011) demonstrated that SGD is a source of alkalinity to the water-column in the Wadden Sea. Therefore, groundwater exchange processes occurring on larger temporal and spatial scales then flow induced advective exchange also have the potential to deliver TA to coral reef lagoons. In fact, Kleypas and Langdon (2006) postulated that ocean acidification may be buffered against in coral reef ecosystems through the exchange of groundwater. The ability of groundwater to act as a source of TA to coral reef lagoons is highly dependent on the exchange rates with the water-column, which can have large temporal and spatial variation (Lewis, 1987; Burnett et al., 2003; Santos et al., 2012). Determining the sources and sinks of alkalinity to coral

reef ecosystems from groundwater and porewater exchange mechanisms is important in constraining how increasing pCO$_2$ will impact seawater carbonate chemistry within coral reef ecosystems.

The hypothesis of this study is that two groundwater sources will contribute TA to Muri Lagoon, a fringing coral reef lagoon in the Cook Islands. To test this hypothesis, advective, benthic incubations were undertaken to determine the influence of porewater advection on alkalinity fluxes from permeable sediments on short temporal and spatial scales (herein referred to as porewater fluxes). Measurements of ^{222}Rn were also undertaken to determine the input of alkalinity from larger temporal and spatial scale groundwater exchange (herein referred to as SGD or groundwater). While "porewater" and "groundwater" are technically synonymous (i.e., any water in contact with geological materials), the hydrology and oceanography communities tend to refer to porewater as a shallow interstitial water and groundwater as deeper, fresher water (Burnett et al., 2003, 2006). In this paper the term porewater is used to refer to the fluxes obtained from advective, benthic chamber incubations, and groundwater (or SGD) to refer to ^{222}Rn-derived fluxes.

2 Materials and methods

2.1 Study site

Our study site was located on the island of Rarotonga, a South Pacific, volcanic island within the archipelago of the Cook Islands. Rarotonga is the largest island in the Cook Islands group (67 km^2) and made up of volcanic rocks that are comprised of 42 % to 53 % SiO$_2$ and 2 % to 14 % CaO (Waterhouse et al., 1986). Rarotonga has a rainy (November to April) and dry (May to October) season, with average annual rainfall of 1900 mm y^{-1} (Thompson, 1986). Muri Lagoon is a fringing, coral reef lagoon located along the south western coast of Rarotonga (Fig. 1). The study site was divided into two locations within Muri Lagoon, one where the chamber incubations were performed

and the second where the water-column monitoring station was set up (Fig. 1). The monitoring station consisted of multiple probes and a bilge pump connected to a cinder block roughly 10 m offshore from the low tide mark. The lagoon extended roughly 750 m offshore to the reef crest from our monitoring station (Fig. 1). Muri Lagoon has an average depth of about 1.4 m and covers an area of 1.75 km^2 (Holden, 1992).The flow in MuriLagoon is dominated by wave setup and runs from the reef crest towards shore, and then northeast along the shore towards a channel which opens to the ocean (Holden, 1992). The tidal cycle in Muri Lagoon is semi-diurnal with an average range of 1 m.

Sediment in the lagoon has a hydraulic conductivity of $\sim 17.3\,\mathrm{m}^{-1}\,\mathrm{d}^{-1}$, which equates to a permeability of approximately $1.91 \times 10^{-11}\,\mathrm{m}^2$. Sediment grain size was 5.8 % > 2 mm, 16.5 % between 1–2 mm, 19.4 % between 500 µm–1 mm, 30.6 % between 250 µm–500 µm, 25.0 % between 125 µm–250 µm, 2.5 % between 63 µm–125 µm, and 0.2 % < 63 µm. Visual inspection of the sediments revealed black coloration a few cm below the surface, which is typical of high sulphide concentrations.

2.2 Advective chamber sampling and porewater fluxes

Chambers identical to those described in Glud et al. (2008) and Eyre et al. (2008) were used to measure in situ benthic solute fluxes at three different advection rates. Three chambers were inserted 15 cm into the sediment and enclosed roughly 4 l of overlying seawater during the incubations. Advection was induced within the chambers based on the spinning rate, in rotations per minute (RPM), of the acrylic disk within each chamber (diffusive, 40 RPM, and 60 RPM). In order to maintain a homogenous distribution of solutes within the diffusive chamber it was operated with the disk slowly spinning clockwise for one rotation, then pausing and spinning counter clockwise for one rotation and repeating (Glud et al., 2008). Incubations were run concurrent with the water-column sampling, starting at 07:00 h on 17 March 2012 and lasting for 28.5 h. Samples of 150 ml were drawn by syringe with ambient seawater allowed to replace the sample volume. Flux rates from the chambers were calculated dusing the integral-based

technique as described in Cyronak et al. (2013). Negative numbers represent a flux into the sediments while positive numbers represent fluxes of solutes out of the sediments. In order to compare advective flux rates to ^{222}Rn derived SGD flux rates, averages between the advective chambers were used (discussed in detail later).

2.3 Water-column sampling

Discrete samples were taken every 2 h from the water-column along with the monitoring of the physico-chemical parameters every 5 min using a multi-probe. A Hydrolab DS5X (Hach Environmental) was deployed 0.2 m from the bottom and 10 m offshore of the low tide mark to monitor temperature ($\pm 0.5\%$), PAR ($\pm 5\%$), and salinity ($\pm 0.5\%$) every 5 min. Depth was measured using an In-Situ Inc. Aqua Troll 200. For the monitoring data, a moving average period of 3 was used over half hour intervals. Sampling of the water-column started at 07:00 h on 17 March 2012 and lasted for 28.5 h. Discrete water samples were taken using 150 ml plastic syringes and brought back to lab to measure salinity, DO, TA, δ^{13}C DIC, and pH.

In order to measure ^{222}Rn concentrations in the water-column, a submersible bilge pump continuously pumped seawater to an onshore gas equilibration device (GED) at about 2 l min^{-1}. The GED equilibrates gas through a shower head exchanger similar to that described in Burnett et al. (2001). Air was recirculated through a closed loop from the GED into a RAD7 radon detector in order to monitor ^{222}Rn concentrations every 30 min (Burnett et al., 2001). In order to generate a groundwater end member for ^{222}Rn derived flux calculations, a bore was dug 10 m onshore of the high tide mark and piezometers were inserted to depths of 1 m and 2.5 m. Discrete samples were taken from the 1 m piezometer at 3 separate times during a diel cycle and one sample was taken from the 2.5 m piezometer. To measure the ^{222}Rn end member of groundwater, a peristaltic pump was used to pump water from the piezometers at 1 l min^{-1} into the GED. The ^{222}Rn was allowed to equilibrate then measured for 1–4 h with the average concentration during that time used as the groundwater end member.

We used a non-steady state radon mass balance model from Burnett and Dulaiova (2003) to determine groundwater flux rates in $cm^3 m^{-2} d^{-1}$. The model incorporated sources of ^{222}Rn from groundwater and ^{226}Ra decay balanced by losses due to atmospheric evasion as a function of wind speed, mixing, and radioactive decay. The alkalinity of the mixed endmember (discussed in detail later) was multiplied by the flux rates generated by the model in order to get ^{222}Rn derived fluxes of groundwater TA into the lagoon.

2.4 Sample analysis

Both water-column and benthic chamber samples were immediately brought back into the laboratory. Dissolved oxygen (±1 %) was measured directly following collection using a Hach Luminescent Dissolved Oxygen (LDO[®]) probe. Samples for nutrients were filtered with a 0.45 μm cellulose acetate filter and frozen at −20 °C until analysed following the methods of Eyre and Ferguson (2005) using a Lachat Flow Injection Analysis (FIA) system. Samples for total alkalinity (TA) and pH were filtered through a 0.45 μm cellulose acetate filter and stored in an airtight container with no headspace until analysis within 4 h of sampling. pH (±0.003) was measured using a Metrohm Electrode Plus calibrated to Oakton National Bureau of Standards (NBS) standards of 4, 7, and 10. To determine TA, Gran titrations were performed using a Metrohm Titrando automatic titrator and pH electrode. Pre-standardized 0.01 mol l^{-1} HCl was used as the titrant which was calibrated against Dickson Certified Reference Material (Batch 111). Alkalinity samples were run twice and the average of the two values was used. During the study the % CV of duplicate TA measurements was 0.15 %.

Samples for $\delta^{13}C$ DIC (±1.2 %) were 0.7 μm filtered with a Whatman GF/F syringe filter, preserved using 50 μl of saturated $HgCl$ with no head space, and stored at 4 °C. Samples were acidified with 5 % ($v : v$) phosphoric acid and the resulting CO_2 was analysed via continuous flow wet-oxidation isotope ratio mass spectrometry (CF-WO-IRMS) using an Aurora 1030 W total organic carbon (TOC) analyzer coupled to a

Thermo Delta V Plus IRMS (Oakes et al., 2010). DIC concentrations were estimated with the Excel macro CO_2 System (CO2SYS) (Pierrot et al., 2006) using inputs of TA and pH and the constants from Mehrbach et al. (1973) refit by Dickson and Millero (1987), CO2SYS also generated Ω_{Ar}. Data from Cyronak et al. (2013) showed excellent agreement between measured and calculated DIC concentrations using the same inputs into CO2SYS as this study. Carbonate alkalinity (TA_C) for the chamber samples was calculated by subtracting the alkalinity, as determined in CO2SYS, contributed by $B(OH)_4^-$, OH^- and total dissolved phosphorus (TDP) from TA.

3   Results

3.1   Advective chambers

The flux rates of TA_C, DIC, DO, and H^+ from the chambers are shown in Fig. 2. All of the rates follow a distinct diel pattern that is consistent with biological activity acting as the driver of solute fluxes from permeable sediments. Flux rates of TA_C decreased throughout the day and began to increase in the late afternoon (Fig. 2a). TA_C flux rates became positive around sunset and increased until midnight, and then varied slightly for the rest of the night until becoming negative in the morning. DIC flux rates showed a similar pattern to TA_C (Fig. 2b). DO and H^+ flux rates followed the opposite pattern of DIC and TA_C fluxes (Fig. 2). DO fluxes increased throughout the morning then decreased in the late afternoon, becoming negative around sunset and levelling off for the night (Fig. 2c). H^+ fluxes showed the same trend as DO fluxes with slight variation in the night (Fig. 2d). In all cases, the flux rates in the 40 RPM chamber exhibited the largest range over a diel cycle (Fig. 2).

Figure 3 shows the hourly flux rates of TA_C, DIC, and DO plotted against the average photosynthetic active radiation (PAR) measured during the same time as the flux was calculated. All three solutes show a distinct hysteretic pattern, with lower rates of all fluxes in the morning at comparable PAR levels in the afternoon (Fig. 3). The fluxes of

TA_C in the 40 RPM chamber showed the largest variation between the morning and afternoon (Fig. 3).

3.2 Water-column time series

The water-column time series was conducted over two tidal cycles and one diel cycle (Fig. 4). Salinity fluctuated throughout the day and the lowest salinities occurred during the low tides (Fig. 4a, b). DO concentrations and Ω_{Ar} followed a trend that was consistent with diel variation driven by biological processes, and throughout the course of the day Ω_{Ar} varied from 2.3–4.4 (Fig. 4e, f). In contrast, TA had a complex dynamics that was related to both diel and tidal cycles (Fig. 4c). DIC concentration showed a similar trend to TA while the $\delta^{13}C$ of DIC following the opposite trend, decreasing with any increase in [DIC] (Fig. 4d). During sampling, radon concentrations in the water-column varied between $7471\,\mathrm{dpm\,m^{-3}}$ to $16\,040\,\mathrm{dpm\,m^{-3}}$, and were highest during low tides (Fig. 5).

3.3 Groundwater endmembers

Both the groundwater measured from piezometers at 1 m and 2.5 m were fresh but differed in solute composition (Table 1). The water chemistry in the three samples taken from the 1 m well did not vary much between the different sampling times, so we reported the average (see Table 1). The DIC concentrations were about twice as high in the shallower groundwater than in the deeper groundwater while $\delta^{13}C$ DIC was more enriched in the deeper groundwater. TA was $7134\,\mathrm{\mu mol\,l^{-1}}$ in the shallow groundwater and $3989\,\mathrm{\mu mol\,l^{-1}}$ in the deeper groundwater. However, radon concentrations showed the opposite trend of the solutes, with concentrations in the deeper groundwater roughly 6 times higher than in the shallow groundwater. The pH of the shallow groundwater was lower than the deeper groundwater.

4 Discussion

4.1 Diel cycling of TA in advective chambers

Hourly flux rates of TA_C, DIC, DO, and H^+ followed trends that were consistent with biological activity driving the fluxes of those solutes over a diel cycle (Fig. 2). During the day, flux rates of all solutes were greatest, whether negative or positive, in the afternoon at the 3:30 h sampling point (Fig. 2). This is consistent with the availability of PAR driving rates of benthic photosynthesis, which would alter the chemistry of porewaters in the permeable sediments thereby affecting both flux rates of TA_C and H^+ (Cook and Røy, 2006; Cyronak et al., 2013). Effluxrates of TA_C in the morning indicate that dissolution of carbonates is still occurring until the late morning when the system shifts to TA_C uptake. During the night time, the flux rates of all solutes tended to level off after the transition between light and dark (Fig. 2). This is probably due to the shift in biological activity from production to respiration and the associated change in porewater chemistry.

Maximum hourly TA_C uptake and efflux rates were highest in the 40 RPM chamber and similar in the diffusive and 60 RPM chambers (Table 2). When compared to flux rates obtained from identical chambers in Heron Island (Australia), fluxes from the Cook Islands were generally lower (Table 2). Uptake rates were stimulated by advection in Heron Island, whereas TA_C uptake rates in the Cook Islands decreased in the highest stirring rate. The exact mechanisms behind these differences are unknown, but visual inspection of the two sediments revealed less biota (e.g. calcareous algae and fauna) in the Cook Island sediments. Lower amounts of benthic fauna would decrease any biologically driven stimulatory effect of advection on benthic fluxes (Cook and Røy, 2006; Cyronak et al., 2013). In addition, the black reducing layer apparent in the Cook Island sediments was not present in Heron Island. As advection delivers oxygen to this layer it may lower the TA concentrations in the porewaters due to sulphide oxidation (Ku et al., 1999). This is consistent with reduced benthic fluxes in the 60 RPM chamber, which would deliver oxygen deepest into the sediments. Grain size

of the sediment was generally smaller in the Cook Islands, with the highest percentage between 250 µm–500 µm compared to Heron which was mostly in the 1–2 mm range. Even though permeability was similar (Glud et al., 2008), differences in grain size may affect the flow of water through the sediments and subsequent TA fluxes. Daily fluxes of TA from the sediments ranged from −1.55 to 7.76 mmol m^{-2} d^{-1}, with the highest rates in the 40 rpm chamber (Table 2).Daily Cook Island TA$_C$fluxes are lower than flux rates in Heron Island, although the daily TA$_C$ flux rate from the 40 RPM chambers are similar in magnitude.

The hysteretic pattern of solute fluxes in the advective chambers is indicative of processes in the sediments being influenced by the previous state of the system (Fig. 3). Lower fluxes in the morning then in the afternoon for TA, DIC, and DO may be due to the decrease in DO and Ω_{Ar} overnight and subsequent change in the system as photosynthesis increases DO in the pore waters (Cyronak et al., 2013). Similar patterns in coral photosynthesis and calcification have been observed over a diel cycle (Levy et al., 2004; Schneider et al., 2009). Levy et al. (2004) attributed the lower photosynthesis rates in the morning to a breakdown of photosynthetic machinery at night and subsequent build-up during the day, while the hysteresis in calcification rates were attributed to changes in respiration rates of corals at specific times during a diel cycle (Schneider et al., 2009). Similar processes may be occurring in the microbiota living in the sediments as well, which would contribute to the observed hysteresis. Also, because DO is consumed through sulphide oxidation (Ku et al., 1999), high sulphide production and the subsequent build-up in the porewaters overnight might also lead to the observed hysteresis in flux rates. If sulphide concentrations built up overnight, DO produced in the morning would be consumed in the sediments, potentially leading to the lower oxygen efflux rates observed in the morning (Fig. 3).

The slope of DIC vs. TA$_C$ can be used to determine the amount of DIC that was produced due to organic or inorganic processes (Gattuso et al., 1996; Andersson and Gledhill, 2013). DIC and TA$_C$ fluxes in the chambers were tightly correlated with an R^2 of 0.970 (Fig. 6a). The organic to inorganic ratio of the DIC flux was 2.13 as calculated

from the slope in Fig. 6a. This value is lower than those reported from water-column measurements but typical of sediments, possibly due to sediment porewaters being in close contact to a non-organic source (i.e. carbonates) of DIC (Gattuso et al., 1996; Cyronak et al., 2013). TA flux rates were not as well correlated to DO fluxes (Fig. 6b) as DIC fluxes corrected for the contribution of TA due to carbonate precipitation and dissolution (Fig. 6c). This may be related to oxygen consumption by sulphides in the sediments (Ku et al., 1999). Additional investigations on the role sulphides play in alkalinity cycling on coral reefs are warranted.

4.2 Estimating a mixed groundwater end member

When plotted against salinity, DIC concentrations in the water-column showed a significant linear correlation consistent with conservative mixing between groundwater and the water-column (Fig. 7). A Keeling plot, or the linear regression of δ^{13}C DIC versus 1/[DIC], can be used to estimate the δ^{13}C of DIC added to the system by calculating the y-intercept (Fig. 8) (Mortazavi and Chanton, 2004; Köhler et al., 2006; Hu and Burdige, 2007). The contribution of both groundwater end members (shallow and deep) to the water-column can be estimated by using the δ^{13}C of added DIC generated from the Keeling plot as the δ^{13}C of the mixed end member. The estimated contribution of the shallow and deep endmembers to the water-column was 47 % and 53 %, respectively (Table 1). The concentrations of DIC, TA, ^{222}Rn, and pH calculated using the above percentages were used as the end member in subsequent mixing models, which matched well to the measured pore water values in the bores (Table 1).

A two-source mixing model can be used to estimate the water-column concentrations of TA based on radon concentrations measured over the sampling period. Radon concentrations from the water-column were divided by the mixed end member concentration (47 % EM1 : 53 % EM2), and a percent groundwater input were then multiplied by the end member of TA (Table 1). When a range of end members was used for the water-column TA, which would change over the course of a day due to biological and geochemical activities (Gattuso et al., 1996; Shamberger et al., 2011), the measured

concentration of TA fit within that range (Fig. 9a). A variable end member model was also calculated based on the change in TA over the course of a day estimated from Fig. 10. During the day, ^{222}Rn versus TA showed a different linear slope than during the night, which is consistent with carbonate precipitation being dominant during the day and dissolution during the night (Fig. 10). The initial concentration in the morning for the water-column TA was estimated as the y-intercept from the night regression of TA vs. ^{222}Rn (2327 mmol l^{-1}). Based on the difference between the y-intercepts for the night and day linear regressions (Fig. 10), an average rate in change of TA in the water-column that excludes the effects of groundwater was estimated as -20 mmol m^{-2} h^{-1} during the day and 20 mmol m^{-2} h^{-1} at night. When the variable end member was applied to the water-column portion of the radon mixing model, there was good agreement between the predicted and measured water-column TA concentrations (Fig. 9b). Observed variability between the measured and predicted water-column TA is probably due to diel variability in TA fluxes that are not accounted for in this model.

Because δ^{13}C of DIC is depleted in the groundwater ($-6\permil$ to $-10\permil$) when compared to oceanic water (0‰ to 2‰) (Williams et al., 2011), and most of the TA in the groundwater is present as DIC, sources of TA to the groundwater can be inferred. The low δ^{13}C values of DIC in the groundwater are indicative of an organic source of carbon, as carbonate minerals tend to have δ^{13}C values from 0‰ to 2‰ (Weber and Woodhead, 1969; Eadie and Jeffrey, 1973; Ogrinc et al., 2003). In addition, a potential uncoupling of sulphate reduction from sulphide oxidation would generate carbonate alkalinity with a depleted δ^{13}C value due to the organic C source, perhaps reflecting the depleted δ^{13}C DIC values found in the groundwater (Ku et al., 1999).

4.3 ^{222}Rn derived TA groundwater fluxes

Advection rates of groundwater into the water-column were estimated using a non-steady state ^{222}Rn mass balance model (Burnett and Dulaiova, 2003) and the concentration of ^{222}Rn estimated in the groundwater endmember (179 202 dpm m^{-3}) (Table 1). Fluxes of groundwater ranged from 0–46 cm d^{-1} and were highest during low tides

(Fig. 11a). This is consistent with tidal pumping driving groundwater flow into the lagoon (Chanton et al., 2003; Kuan et al., 2012). The groundwater flux rates can be converted to an hourly basis and multiplied by the groundwater end member concentration of TA ($5467\,\mu mol\,l^{-1}$) to estimate the fluxes of TA into the water-column (Fig. 11b). Fluxes ranged from $0–105\,mmol\,m^{-2}\,h^{-1}$ over a tidal cycle, with the highest fluxes observed during the lowest tides.

There are a number of factors that would influence the flux of TA from SGD into coastal ecosystems, one of which is the concentration of TA in the groundwater. In general TA concentrations of groundwater exhibit a large range and are probably highly dependent on local geology, but can be up to 6 times as high as oceanic TA (Table 3). Also, the amount of TA fluxed into the lagoon is dependent on how far the groundwater mixes offshore and the location of point-sources of SGD within the lagoon (Burnett et al., 2003; Burnett and Dulaiova, 2003; Schopka and Derry, 2012). Based on radium isotope ratios in Muri Lagoon, a conservative residence time of 6 days was estimated for water in the lagoon (Tait et al., 2012). This long residence time means TA derived from groundwater can act as a potential source of carbonates to the lagoon, raising the Ω_{Ar} of the lagoon above oceanic levels and helping to buffer against ocean acidification. However, groundwater may also act as a source of CO_2, which would inhibit the buffering capacity of SGD associated TA fluxes. Also, groundwater is a potential source of nutrients (Valiela et al., 1999; Burnett et al., 2003; Paytan et al., 2006), contaminants (Cohen et al., 1984; Bedient et al., 1994), and other solutes that could potentially degrade reef health.

There are not many studies assessing the influence of SGD on alkalinity fluxes to the water-column, and none in coral reef ecosystems. Moore et al. (2011) used radium isotopes to trace the fluxes of groundwater to the Wadden Sea, showing that SGD acts as an important source of TA, Mn, dissolved organic carbon (DOC), and silicate to the ocean. Other studies have measured the concentration of TA in groundwater, but do not discuss SGD fluxes of TA to open water ecosystems (see Table 3). There are multiple exchange processes of groundwater that could alter TA fluxes to the

water-column besides terrestrial hydraulic gradient driven SGD (Burnett et al., 2003; Santos et al., 2012). For instance, tidal pumping and saltwater intrusion occurring on a larger scale then advective process may alter microbial processes in the sediment,and subsequently the cycling of TA (Kuan et al., 2012; Santos et al., 2012). The impact of these processes on TA fluxes into coral reef lagoons merits further investigation.

4.4 Upscaling porewater and groundwater fluxes

In order to compare the two sources of groundwater and their influence on TA concentrations in the lagoon, a 750 m × 1 m transect was projected from the sampling site to the reef crest (Fig. 1). Since chamber stirring rates did not show any major influence on alkalinity fluxes from sediments, an average hourly flux rate from the two advective chambers (40 and 60 RPM) was used for this comparison. SGD was conservatively assumed to occur within a horizontal seepage face of 50 m from the beach face, as suggested from resistivity transects (Tait et al., 2012). The fluxes of TA associated with advective processes were both negative and positive while the groundwater fluxes were always positive (Fig. 12). SGD contributed 27 % to 97 % of the combined groundwater fluxes over a diel cycle, with the percent contribution dependant on both the time of day and the tidal cycle (Fig. 12). Since groundwater seepage is correlated to tidal height (Chanton et al., 2003), larger tides would have more of an effect on groundwater flow, potentially allowing more TA to be fluxed into the system during those tidal cycles. However, because advective processes follow a diel cycle and groundwater is driven by tidal cycles, it becomes complex to determine which of the processes is more influential over the long term.

Across the 750 m transect, groundwater (from both porewater advection and SGD) contributes 46.3 to 52.8 mol TA d^{-1} to the water-column. Based off of satellite images and dark coloration along the transect we estimate coralcover of about 22 %, which is probably an over-estimate as not all dark benthos is necessarily coral. Assuming that the coral uptakes TA at a rate of 400 mmol m^{-2} d^{-1} (Gattuso et al., 1996; Nakamura and Nakamori, 2009), then groundwater processes would contribute 70 % to 80 % of

TA used by corals. This represents a large portion of the TA consumed by corals in the lagoon, although residence time and circulation patterns will play large roles in how much of the groundwater derived TA would be available to corals. In order to estimate the percent that groundwater derived TA contributes to the molar amount of TA that is present in the lagoon water-column we assumed a steady state concentration of $2300\,\mu\mathrm{mol\,l^{-1}}$. This equates to 2415 moles of TA, of which groundwater derived TA contributes 11 % to 13 % based on a 6 day residency time. This previously unaccounted for TA is important in changing the carbon chemistry within Muri Lagoon over tidal and diel cycles.

5   Conclusions

Alkalinity concentrations in Muri Lagoon followed a pattern that is indicative of both biological and tidal drivers influencing the dynamics of water-column TA over a diel cycle (Fig. 4). Different groundwater exchange mechanisms, acting on varying temporal and spatial scales can have different influences on water-column alkalinity. TA fluxes related to small scale porewater advection acted as both a source and sink of TA over the course of a day, with net daily fluxes ranging from -1.55 to $7.76\,\mathrm{mmol\,m^{-2}\,d^{-1}}$ depending on advection rates. SGD fluxes were driven by tidal processes and delivered $1080\,\mathrm{mmol\,TA\,m^{-2}\,d^{-1}}$ to the water-column over the course of this study. It is likely that similar advective exchanges of TA occur throughout different reef systems, while SGD is highly dependent on the specific geological, physical, and biological attributes of the land masses associated with coral reefs. Overall, it is important to constrain groundwater exchange processes occurring in coral reef ecosystems so that more detailed models predicting how ocean acidification will alter reef carbonate chemistry can be developed.

References

Andersson, A. J., Bates, N., and Mackenzie, F.: Dissolution of carbonate sediments under rising PCO$_2$ and ccean acidification: Observations from Devil's Hole, Bermuda, Aquat. Geochem., 13, 237–264, doi:10.1007/s10498-007-9018-8, 2007.

Andersson, A. J. and Gledhill, D.: Ocean acidification and coral reefs: Effects on breakdown, dissolution, and net ecosystem calcification, Annual Review of Marine Science, 5, null, doi:10.1146/annurev-marine-121211-172241, 2013.

Andersson, A. J. and Mackenzie, F. T.: Revisiting four scientific debates in ocean acidification research, Biogeosciences, 9, 893–905, doi:10.5194/bg-9-893-2012, 2012.

Bedient, P. B., Rifai, H. S., and Newell, C. J.: Ground water contamination: transport and remediation, Prentice-Hall International, Inc., 1994.

Burnett, W. C. and Dulaiova, H.: Estimating the dynamics of groundwater input into the coastal zone via continuous radon-222 measurements, J. Environ. Radioact., 69, 21–35, 2003.

Burnett, W., Kim, G., and Lane-Smith, D.: A continuous monitor for assessment of 222Rn in the costal ocean, J. Radioanal. Nucl. Ch., 249, 167–172, 2001.

Burnett, W. C., Bokuniewicz, H., Huettel, M., Moore, W. S., and Taniguchi, M.: Groundwater and pore water inputs to the coastal zone, Biogeochemistry, 66, 3–33, doi:10.1023/b:biog.0000006066.21240.53, 2003.

Burnett, W., Aggarwal, P., Aureli, A., Bokuniewicz, H., Cable, J., Charette, M., Kontar, E., Krupa, S., Kulkarni, K., and Loveless, A.: Quantifying submarine groundwater discharge in the coastal zone via multiple methods, Sci. Total Environ., 367, 498–543, 2006.

Cable, J., Burnett, W., Chanton, J., and Weatherly, G.: Modeling groundwater flow into the ocean based on 222Rn, Earth Planet. Sc. Lett., 144, 591–604, 1996.

Cai, W. J., Wang, Y., Krest, J., and Moore, W.: The geochemistry of dissolved inorganic carbon in a surficial groundwater aquifer in North Inlet, South Carolina, and the carbon fluxes to the coastal ocean, Geochim. Cosmochim. Acta, 67, 631–639, 2003.

Chanton, J. P., Burnett, W. C., Dulaiova, H., Corbett, D. R., and Taniguchi, M.: Seepage rate variability in Florida Bay driven by Atlantic tidal height, Biogeochemistry, 66, 187–202, 2003.

Groundwater and porewater as a major source of alkalinity

T. Cyronak et al.

Title Page	
Abstract	Introduction
Conclusions	References
Tables	Figures
◄◄	►►
◄	►
Back	Close
Full Screen / Esc	

Printer-friendly Version

Interactive Discussion

Chisholm, J. R. M. and Gattuso, J.-P.: Validation of the alkalinity anomaly technique for investigating calcification and photosynthesis in coral reef communities, Limnol. Oceanogr., 36, 1232–1239, 1991.

Cohen, S., Creeger, S., Carsel, R., and Enfield, C.: Potential pesticide contamination of groundwater from agricultural uses, 297–325, 1984.

Cook, P. L. M. and Røy, H.: Advective relief of CO_2 limitation in microphytobenthos in highly productive sandy sediments, Limnol. Oceanogr., 51, 1594–1601, 2006.

Cyronak, T., Santos, I., McMahon, A., and Eyre, B. D.: Carbon cycling hysteresis in permeable carbonate sands over a diel cycle: Implications for ocean acidification, Limnol. Oceanogr., in press, 2013.

D'Elia, C. F. and Wiebe, W. J.: Biogeochemical nutrient cycles in coral-reef ecosystems, Ecosystems of the world, 25, 49–74, 1990.

De'ath, G., Lough, J. M., and Fabricius, K. E.: Declining coral calcification on the Great Barrier Reef, Science, 323, 116–119, doi:10.1126/science.1165283, 2009.

Dickson, A. and Millero, F.: A comparison of the equilibrium constants for the dissociation of carbonic acid in seawater media, Deep Sea Res., 34, 1733–1743, 1987.

Doney, S. C., Fabry, V. J., Feely, R. A., and Kleypas, J. A.: Ocean acidification: the other CO_2 problem, Annual Review of Marine Science, 1, 169–192, 2009.

Eadie, B. J. and Jeffrey, L. M.: d13C analyses of oceanic particulate organic matter, Mar. Chem., 1, 199–209, 1973.

Eyre, B. D. and Ferguson, A. J. P.: Benthic metabolism and nitrogen cycling in a subtropical east Australian estuary (Brunswick): Temporal variability and controlling factors, Limnol. Oceanogr., 50, 81–96, 2005.

Eyre, B. D., Glud, R. N., and Patten, N.: Mass coral spawning: A natural large-scale nutrient addition experiment, Limnol. Oceanogr., 53, 997–1013, 2008.

Fabry, V. J., Seibel, B. A., Feely, R. A., and Orr, J. C.: Impacts of ocean acidification on marine fauna and ecosystem processes, ICES J. Ma. Sci.: J. Conseil, 65, 414–432, 2008.

Feely, R. A., Sabine, C. L., Lee, K., Berelson, W., Kleypas, J., Fabry, V. J., and Millero, F. J.: Impact of anthropogenic CO_2 on the $CaCO_3$ system in the oceans, Science, 305, 362–366, doi:10.1126/science.1097329, 2004.

Frankignoulle, M., Gattuso, J. P., Biondo, R., Bourge, I., Copin-Montégut, G., and Pichon, M.: Carbon fluxes in coral reefs. II. Eulerian study of inorganic carbon dynam-

ics and measurement of air-sea CO2 exchanges, Mar. Ecol. Prog. Ser., 145, 123–132, doi:10.3354/meps145123, 1996.

Gattuso, J., Pichon, M., Delesalle, B., Canon, C., and Frankignoulle, M.: Carbon fluxes in coral reefs, I, Lagrangian measurement of community metabolism and resulting air-sea CO_2 disequilibrium, MEPS, 145, 109–121, 1996.

Glud, R. N., Eyre, B. D., and Patten, N.: Biogeochemical responses to mass coral spawning at the Great Barrier Reef: Effects on respiration and primary production, Limnol. Oceanogr., 53, 1014–1024, 2008.

Gray, S. E. C., DeGrandpre, M. D., Langdon, C., and Corredor, J. E.: Short-term and seasonal pH, pCO_2 and saturation state variability in a coral-reef ecosystem, Global Biogeochem. Cycles, 26, GB3012, doi:10.1029/2011gb004114, 2012.

Holden, B. J.: Circulation and flushing Ngatangiia harbour and Muri lagoon Rarotonga, Cook Islands, South Pacific Applied Geoscience Commission, 1992.

Hu, X. and Burdige, D. J.: Enriched stable carbon isotopes in the pore waters of carbonate sediments dominated by seagrasses: Evidence for coupled carbonate dissolution and reprecipitation, Geochim. Cosmochim. Acta, 71, 129–144, 2007.

Kim, K., Rajmohan, N., Kim, H. J., Hwang, G. S., and Cho, M. J.: Assessment of groundwater chemistry in a coastal region (Kunsan, Korea) having complex contaminant sources: a stoichiometric approach, Environ. Geol., 46, 763–774, 2004.

Kleypas, J. A. and Langdon, C.: Coral reefs and changing seawater carbonate chemistry, Coastal and Estuarine Studies, 2006, 73, doi:10.1029/61CE06, 2006.

Köhler, P., Fischer, H., Schmitt, J., and Munhoven, G.: On the application and interpretation of Keeling plots in paleo climate research – deciphering $\delta^{13}C$ of atmospheric CO_2 measured in ice cores, Biogeosciences, 3, 539–556, doi:10.5194/bg-3-539-2006, 2006.

Ku, T. C. W., Walter, L. M., Coleman, M. L., Blake, R. E., and Martini, A. M.: Coupling between sulfur recycling and syndepositional carbonate dissolution: evidence from oxygen and sulfur isotope composition of pore water sulfate, South Florida Platform, U.S.A, Geochim. Cosmochim. Acta, 63, 2529–2546, doi:10.1016/s0016-7037(99)00115-5, 1999.

Kuan, W. K., Jin, G., Xin, P., Robinson, C., Gibbes, B., and Li, L.: Tidal influence on seawater intrusion in unconfined coastal aquifers, Water Resour. Res., 48, W02502, doi:10.1029/2011wr010678, 2012.

Lazar, B. and Loya, Y.: Bioerosion of coral reefs-A chemical approach, Limnol. Oceanogr., 36, 377–383, 1991.

Groundwater and porewater as a major source of alkalinity

T. Cyronak et al.

Title Page

Abstract | Introduction

Conclusions | References

Tables | Figures

|◄ | ►|

◄ | ►

Back | Close

Full Screen / Esc

Printer-friendly Version

Interactive Discussion

Levy, O., Dubinsky, Z., Schneider, K., Achituv, Y., Zakai, D., and Gorbunov, M. Y.: Diurnal hysteresis in coral photosynthesis, Mar. Ecol. Prog. Ser., 268, 105–117, 2004.

Lewis, J. B.: Measurements of groundwater seepage flux onto a coral reef: Spatial and temporal variations, Limnol. Oceanogr., 1165–1169, 1987.

Liu, Q., Dai, M., Chen, W., Huh, C.-A., Wang, G., Li, Q., and Charette, M. A.: How significant is submarine groundwater discharge and its associated dissolved inorganic carbon in a river-dominated shelf system?, Biogeosciences, 9, 1777–1795, doi:10.5194/bg-9-1777-2012, 2012.

Mahlknecht, J., Steinich, B., and Navarro de León, I.: Groundwater chemistry and mass transfers in the Independence aquifer, central Mexico, by using multivariate statistics and mass-balance models, Environ. Geol., 45, 781–795, doi:10.1007/s00254-003-0938-3, 2004.

Manzello, D. P., Kleypas, J. A., Budd, D. A., Eakin, C. M., Glynn, P. W., and Langdon, C.: Poorly cemented coral reefs of the eastern tropical Pacific: Possible insights into reef development in a high-CO_2 world, P. Natl. Acad. Sci., 105, 10450–10455, doi:10.1073/pnas.0712167105, 2008.

Mehrbach, C., Culberson, C., Hawley, J., and Pytkowicz, R.: Measurement of the apparent dissociation constants of carbonic acid in seawater at atmospheric pressure, Limnol. Oceanogr., 18, 897–907, 1973.

Millero, F. J.: The thermodynamics of the carbonate system in seawater, Geochim. Cosmochim. Acta, 43, 1651–1661, doi:10.1016/0016-7037(79)90184-4, 1979.

Moore, W., Beck, M., Riedel, T., Rutgers van der Loeff, M., Dellwig, O., Shaw, T., Schnetger, B., and Brumsack, H. J.: Radium-based pore water fluxes of silica, alkalinity, manganese, DOC, and uranium: A decade of studies in the German Wadden Sea, Geochim. Cosmochim. Acta, 75, 6535–6555, 2011.

Morse, J. W., Andersson, A. J., and Mackenzie, F. T.: Initial responses of carbonate-rich shelf sediments to rising atmospheric PCO_2 and "ocean acidification": Role of high Mg-calcites, Geochim. Cosmochim. Acta, 70, 5814–5830, doi:10.1016/j.gca.2006.08.017, 2006.

Mortazavi, B. and Chanton, J. P.: Use of Keeling plots to determine sources of dissolved organic carbon in nearshore and open ocean systems, Limnol. Oceanogr., 49, 102–108, 2004.

Nakamura, T. and Nakamori, T.: Estimation of photosynthesis and calcification rates at a fringing reef by accounting for diurnal variations and the zonation of coral reef communities on reef flat and slope: a case study for the Shiraho reef, Ishigaki Island, southwest Japan, Coral Reefs, 28, 229–250, 2009.

Title Page

Abstract | Introduction

Conclusions | References

Tables | Figures

◀ | ▶

◀ | ▶

Back | Close

Full Screen / Esc

Printer-friendly Version

Interactive Discussion

Oakes, J. M., Eyre, B. D., Ross, D. J., and Turner, S. D.: Stable isotopes trace estuarine trans-formations of carbon and nitrogen from primary- and secondary-treated paper and pulp mill effluent, Environ. Sci. Technol., 44, 7411–7417, doi:10.1021/es101789v, 2010.

Ogrinc, N., Faganeli, J., and Pezdic, J.: Determination of organic carbon remineralization in near-shore marine sediments (Gulf of Trieste, Northern Adriatic) using stable carbon isotopes, Org. Geochem., 34, 681–692, 2003.

Orr, J. C., Fabry, V. J., Aumont, O., Bopp, L., Doney, S. C., Feely, R. A., Gnanadesikan, A., Gruber, N., Ishida, A., and Joos, F.: Anthropogenic ocean acidification over the twenty-first century and its impact on calcifying organisms, Nature, 437, 681–686, 2005.

Paytan, A., Shellenbarger, G. G., Street, J. H., Gonneea, M. E., Davis, K., Young, M. B., and Moore, W. S.: Submarine groundwater discharge: An important source of new inorganic nitrogen to coral reef ecosystems, Limnol. Oceanogr., 51, 343–348, 2006.

Precht, E. and Huettel, M.: Advective pore-water exchange driven by surface gravity waves and its ecological implications, Limnol. Oceanogr., 48, 1674–1684, 2003.

Rad, S. D., Allègre, C. J., and Louvat, P.: Hidden erosion on volcanic islands, Earth Planet. Sc. Lett., 262, 109–124, 2007.

Rao, A. M. F., Polerecky, L., Ionescu, D., Meysman, F. J. R., and de Beer, D.: The influence of pore-water advection, benthic photosynthesis, and respiration on calcium carbonate dynamics in reef sands, Limnol. Oceanogr., 57, 809–825, 2012.

Sabine, C. L., Feely, R. A., Gruber, N., Key, R. M., Lee, K., Bullister, J. L., Wanninkhof, R., Wong, C. S., Wallace, D. W. R., Tilbrook, B., Millero, F. J., Peng, T.-H., Kozyr, A., Ono, T., and Rios, A. F.: The Oceanic Sink for Anthropogenic CO_2, Science, 305, 367–371, doi:10.1126/science.1097403, 2004.

Santos, I. R., Machado, M. I., Niencheski, L. F., Burnett, W., Milani, I. B., Andrade, C. F. F., Peterson, R. N., Chanton, J., and Baisch, P.: Major ion chemistry in a freshwater coastal lagoon from southern Brazil (Mangueira Lagoon): Influence of groundwater inputs, Aquat. Geochem., 14, 133–146, 2008.

Santos, I. R., Glud, R. N., Maher, D., Erler, D., and Eyre, B. D.: Diel coral reef acidification driven by porewater advection in permeable carbonate sands, Heron Island, Great Barrier Reef, Geophys. Res. Lett., 38, L03604, doi:10.1029/2010gl046053, 2011.

Santos, I. R., Eyre, B. D., and Huettel, M.: The driving forces of porewater and groundwater flow in permeable coastal sediments: A review, Estuar. Coast. Shelf Sci., 98, 1–15, doi:10.1016/j.ecss.2011.10.024, 2012.

Groundwater and porewater as a major source of alkalinity

T. Cyronak et al.

Title Page

Abstract | Introduction

Conclusions | References

Tables | Figures

◀ | ▶

◀ | ▶

Back | Close

Full Screen / Esc

Printer-friendly Version

Interactive Discussion

Schneider, K., Levy, O., Dubinsky, Z., and Erez, J.: In situ diel cycles of photosynthesis and calcification in hermatypic corals, Limnol. Oceanogr., 54, 1995–2002, 2009.

Schopka, H. H. and Derry, L. A.: Chemical weathering fluxes from volcanic islands and the importance of groundwater: The Hawaiian example, Earth Planet. Sc. Lett., 339, 67–78, 2012.

Shamberger, K. E. F., Feely, R. A., Sabine, C. L., Atkinson, M. J., DeCarlo, E. H., Mackenzie, F. T., Drupp, P. S., and Butterfield, D. A.: Calcification and organic production on a Hawaiian coral reef, Mar. Chem., 127, 64–75, doi:10.1016/j.marchem.2011.08.003, 2011.

Shaw, E. C., McNeil, B. I., and Tilbrook, B.: Impacts of ocean acidification in naturally variable coral reef flat ecosystems, J. Geophys. Res., 117, C03038, doi:10.1029/2011jc007655, 2012.

Silverman, J., Kline, D. I., Johnson, L., Rivlin, T., Schneider, K., Erez, J., Lazar, B., and Caldeira, K.: Carbon turnover rates in the One Tree Island reef: A 40-year perspective, J. Geophys. Res., 117, G03023, doi:10.1029/2012jg001974, 2012.

Suzuki, A. and Kawahata, H.: Carbon budget of coral reef systems: an overview of observations in fringing reefs, barrier reefs and atolls in the Indo-Pacific regions, Tellus B, 55, 428–444, 2003.

Thompson, C. S.: The climate and weather of the southern Cook Islands, New Zealand Meteorological Service, 1986.

Valiela, I., Costa, J., Foreman, K., Teal, J. M., Howes, B., and Aubrey, D.: Transport of groundwater-borne nutrients from watersheds and their effects on coastal waters, Biodegradation, 10, 177–197, 1999.

Waterhouse, B., Petty, D. R., and Mackenzie, I.: Hydrogeology of the Southern Cook Islands, South Pacific, 98, Published for New Zealand Geological Survey by Science Information Pub. Centre, 1986.

Weber, J. N. and Woodhead, P. M. J.: Factors affecting the carbon and oxygen isotopic composition of marine carbonate sediments – II. Heron Island, Great Barrier Reef, Australia, Geochim. Cosmochim. Acta, 33, 19–38, doi:10.1016/0016-7037(69)90090-8, 1969.

Williams, B., Halfar, J., Steneck, R. S., Wortmann, U. G., Hetzinger, S., Adey, W., Lebednik, P., and Joachimski, M.: Twentieth century $\delta^{13}C$ variability in surface water dissolved inorganic carbon recorded by coralline algae in the northern North Pacific Ocean and the Bering Sea, Biogeosciences, 8, 165–174, doi:10.5194/bg-8-165-2011, 2011.

Title Page

Abstract | Introduction

Conclusions | References

Tables | Figures

|◀ | ▶|

◀ | ▶

Back | Close

Full Screen / Esc

Printer-friendly Version

Interactive Discussion

Wolf-Gladrow, D. A., Zeebe, R. E., Klaas, C., Körtzinger, A., and Dickson, A. G.: Total alkalinity: The explicit conservative expression and its application to biogeochemical processes, Mar. Chem., 106, 287–300, 2007.

Zeebe, R. E. and Wolf-Gladrow, D.: CO_2 in seawater: Equilibrium, kinetics, isotopes, Elsevier Oceanography Series, Amsterdam, 2001.

Zundelevich, A., Lazar, B., and Ilan, M.: Chemical versus mechanical bioerosion of coral reefs by boring sponges-lessons from *Pione cf. vastifica*, J. Exp. Biol., 210, 91–96, 2007.

Groundwater and porewater as a major source of alkalinity

T. Cyronak et al.

Full Screen / Esc

Printer-friendly Version

Interactive Discussion

Table 1. Measurements of solutes in the groundwater end members (EM), EM1 $n = 3$, EM2 $n = 1$. δ^{13}C DIC of the mixed endmember was estimated from the y-intercept of a Keeling plot. The 47 % EM1 : 53 % EM2 are concentrations calculated from the δ^{13}C DIC estimated end member values.

	Depth (m)	DIC (μmol l^{-1})	δ^{13}C DIC	TA (μmol l^{-1})	^{222}Rn (dpm m^{-3})	pH
Ground Water EM1	1	9381 ± 354	−10.12 ± 1.02	7134 ± 60	49 585 ± 1743	7.325
Ground Water EM2	2.5	4251	−6.3	3989	294 146 ± 4601	7.593
47 % EM1 : 53 % EM2	–	6661	−8.09	5467	179 202	7.480

Table 2. Maximum hourly uptake and efflux rates of TA_C measured from advective benthic chambers in this study compared to a similar study on the Great Barrier Reef. Daily flux rates of TA_C are also shown.

Location	Chamber	TA_C Efflux ($\mathrm{mmol\,m^{-2}\,h^{-1}}$)	TA_C Uptake ($\mathrm{mmol\,m^{-2}\,h^{-1}}$)	Daily TA_C Flux ($\mathrm{mmol\,m^{-2}\,d^{-1}}$)	Source
Cook Islands	Diffusive	3.32	−4.01	−1.16	This study
	40 RPM	3.96	−4.78	7.76	
	60 RPM	3.17	−4.01	−1.55	
Heron Island	Diffusive	5.21	−4.83	5.13	Cyronak et al. (2013)
	40 RPM	4.93	−5.65	8.84	
	80 RPM	5.61	−7.36	8.78	

Table 3. Concentrations of TA (μmol l^{-1}) measured in groundwater throughout the world. [*] Designates concentrations measured as HCO_3^-.

TA (umol l^{-1})	System type	Location	Reference
2150–2949	Subtropical estuary	South Carolina, USA	Cai et al. (2003)
90–8920	Subtropical estuary	Kunsan, Korea	Kim et al. (2004)
4.020	Subtropical estuary	Southern China	Liu et al. (2012)
753–7026[*]	Inland mountains	Central Mexico	Mahlknecht et al. (2004)
2550–23 300	Tidal flat	Wadden Sea, Germany	Moore 2011
95–2000[*]	Tropical island	Guadeloupe	Rad et al. (2007)
1400–13 000[*]	Tropical island	Martinique	Rad et al. (2007)
800–4016[*]	Tropical island	Reunion	Rad et al. (2007)
2290[*]	Coastal lagoon	Brazil	Santos et al. (2008)
1.32–2162	Tropical island	Hawaii	Schopka and Derry (2012)
3989–7134	Tropical island	Cook Islands	This study
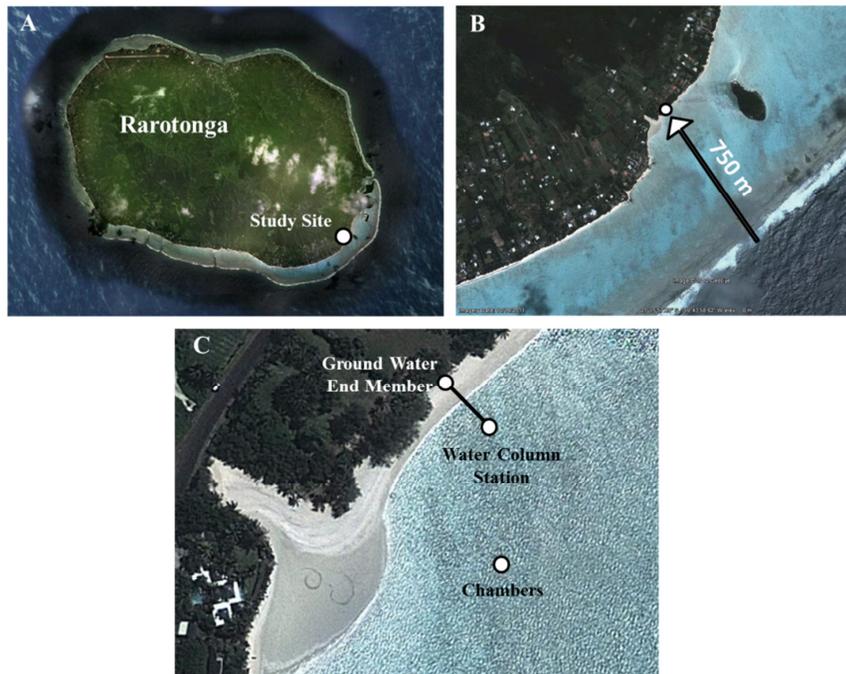
Fig. 1. A map of Rarotonga showing the location of Muri Lagoon and the sampling site.
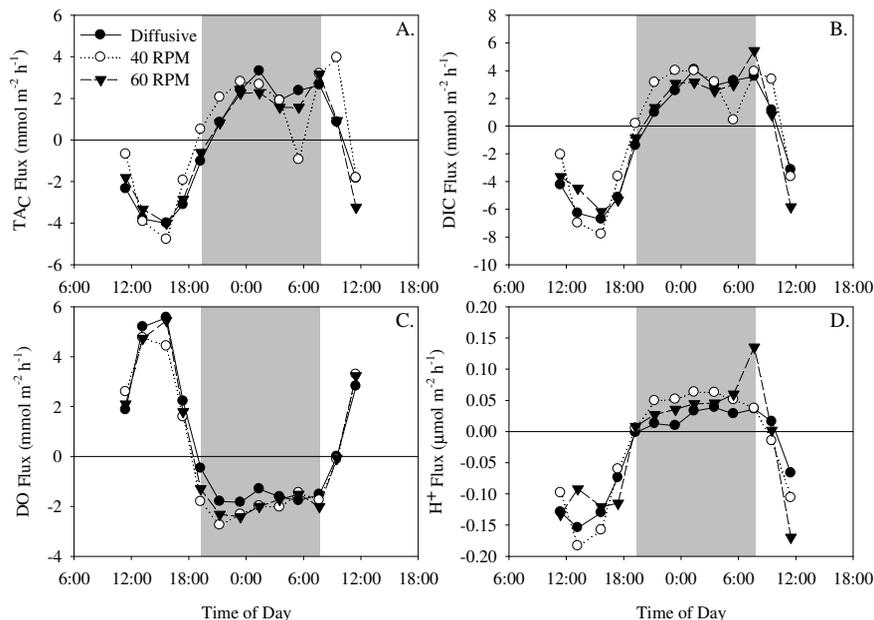
Fig. 2. Hourly, integral derived flux rates of TA_C, DIC, DO and H^+ from the advective chambers. Grey bars represent night hours. All fluxes are in mmol m^{-2} h^{-1} besides H^+ which are in μmol m^{-2} h^{-1}.

Full Screen / Esc

Printer-friendly Version

Interactive Discussion
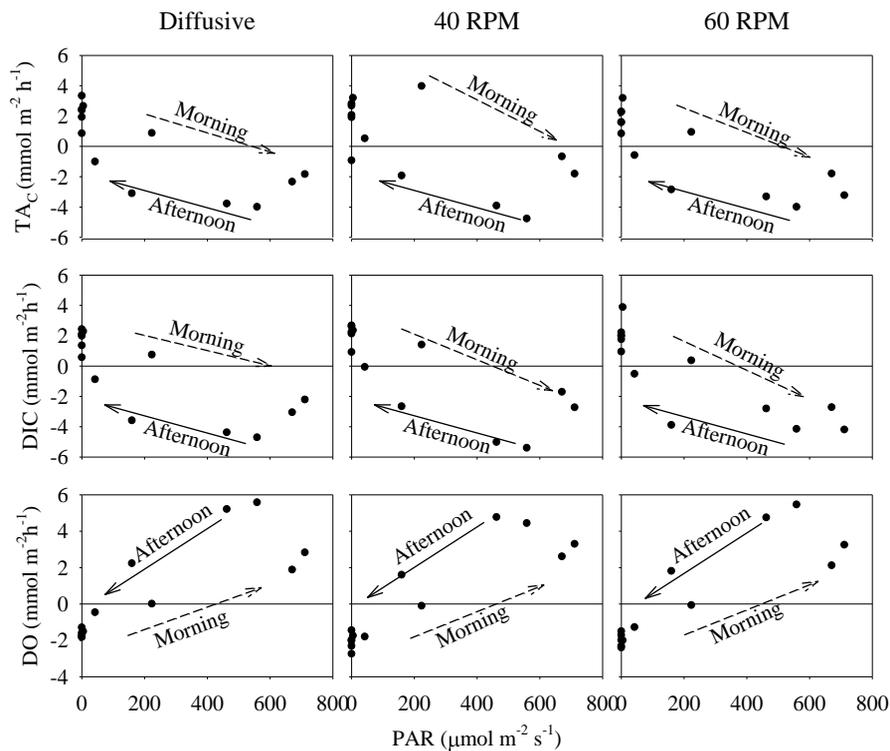
Fig. 3. Flux rates of TA$_C$, DIC, and DO plotted against the average PAR values measured during the same time period as the flux. Flux rates are in mmol m^{-2} h^{-1}.
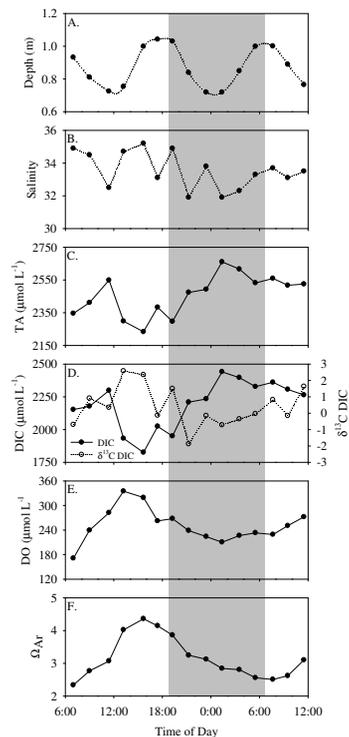
Full Screen / Esc

Fig. 4. (A) Depth, **(B)** salinity, **(C)** TA, **(D)** DIC, **(E)** DO, and **(F)** Ω_{Ar} measured in the discrete water samples taken from the water-column. Grey bars represent night hours.

Full Screen / Esc

Printer-friendly Version

Interactive Discussion

Fig. 5. Radon concentrations and depth measured at the water-column monitoring site over the course of the study.
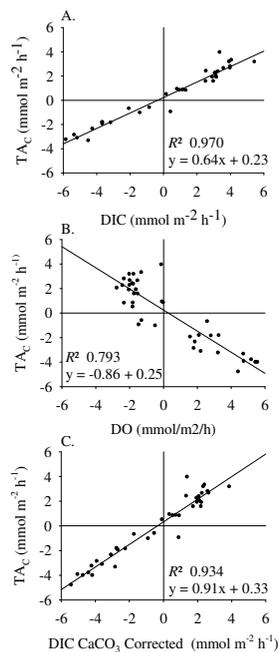
Fig. 6. Linear regressions of **(A)** TA_C vs. DIC, **(B)** TA_C vs. DO, and (C) TA_C vs. DIC corrected for $CaCO_3$ dissolution from all stirring rates of the advective chamber incubations. Equations and R^2 values are displayed for each regression.
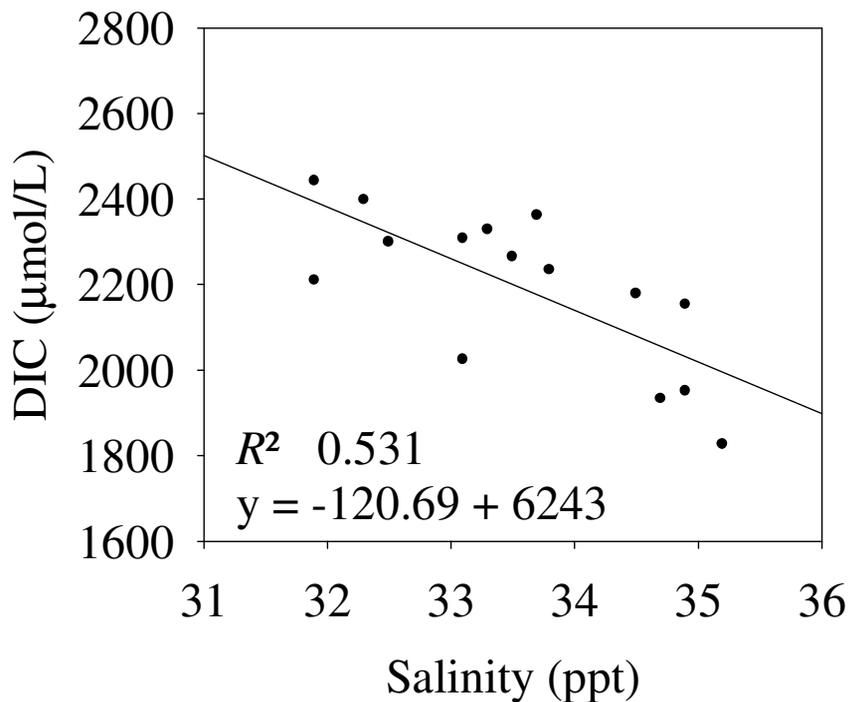
Fig. 7. Regression of salinity vs. concentrations of DIC in the water-column measured over the course of the study. The regression equation and R^2 value are displayed.
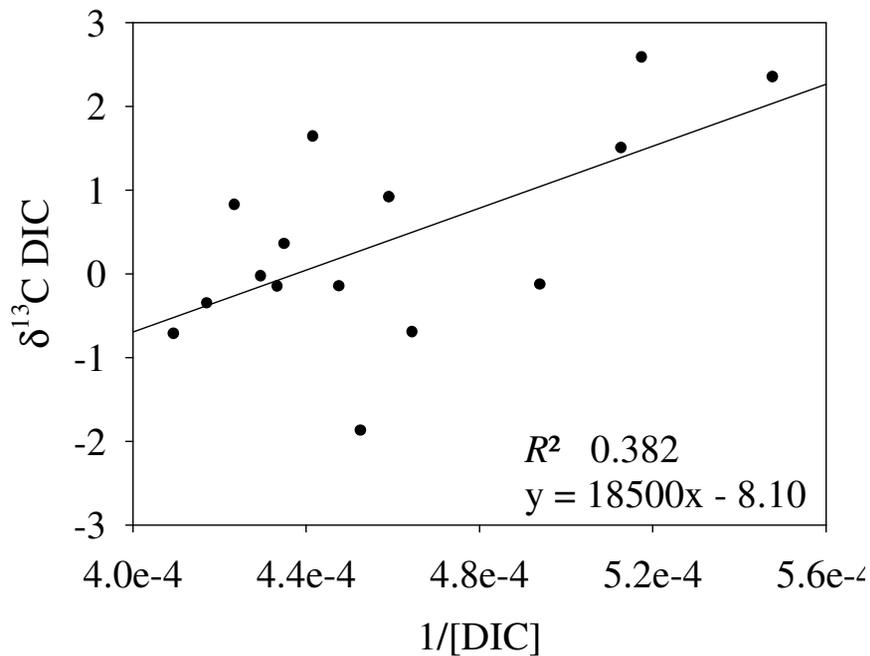
Fig. 8. Keeling plot of δ^{13}C DIC vs. 1/[DIC] measured in the water-column.

Full Screen / Esc

Printer-friendly Version

Interactive Discussion
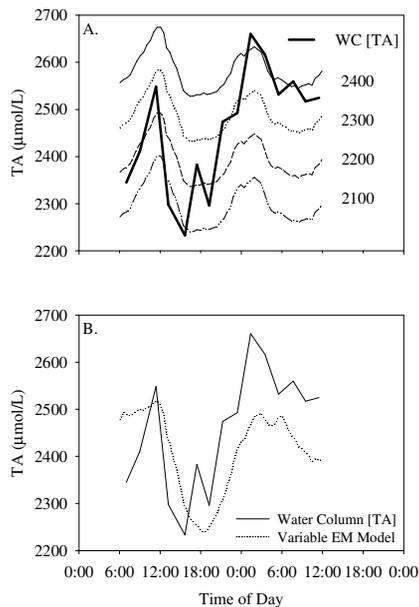
Fig. 9. Concentration of TA in the water-column during the course of the study plotted along with the estimated concentration of TA based on the [222]Rn derived mixing model. **(A)** Four separate mixing models using a range of TA concentrations for the oceanic end member from 2100–2400 μmol l^{-1}, **(B)** the variable oceanic end member model. All TA concentrations are in μmol l^{-1}.

Full Screen / Esc

Printer-friendly Version

Interactive Discussion
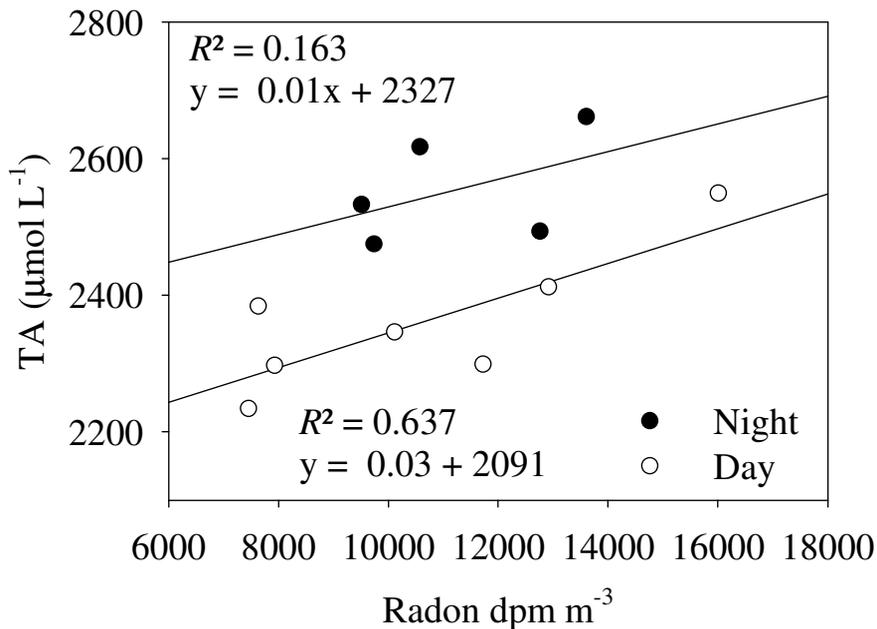
Fig. 10. TA vs. [222]Rn concentrations in the water-column, separate regressions were made for day time and night time hours. The three daylight time points taken during the second sampling day were removed from the regressions.
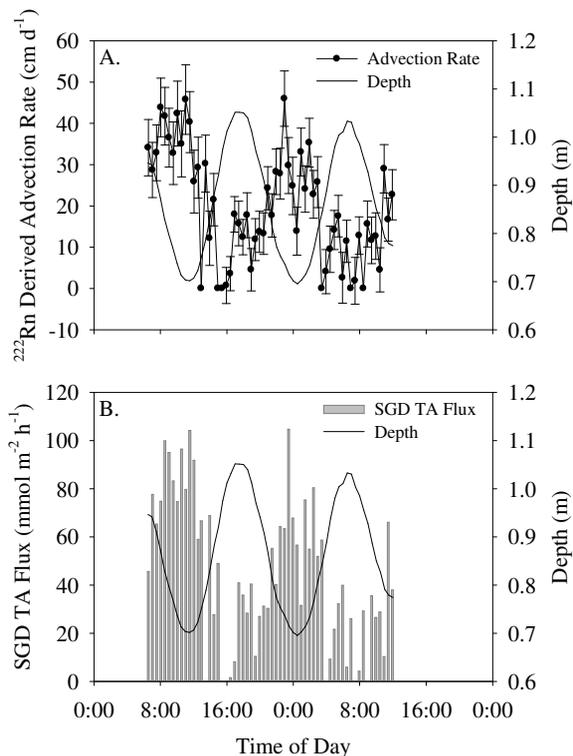
Fig. 11. (A) SGD advection rates in cm d^{-1} estimated using the model from Burnett and Dulaiova (2003) plotted alongside depth measured during the study. **(B)** Hourly SGD derived flux rates of TA into the water-column plotted with depth over the course of the study.
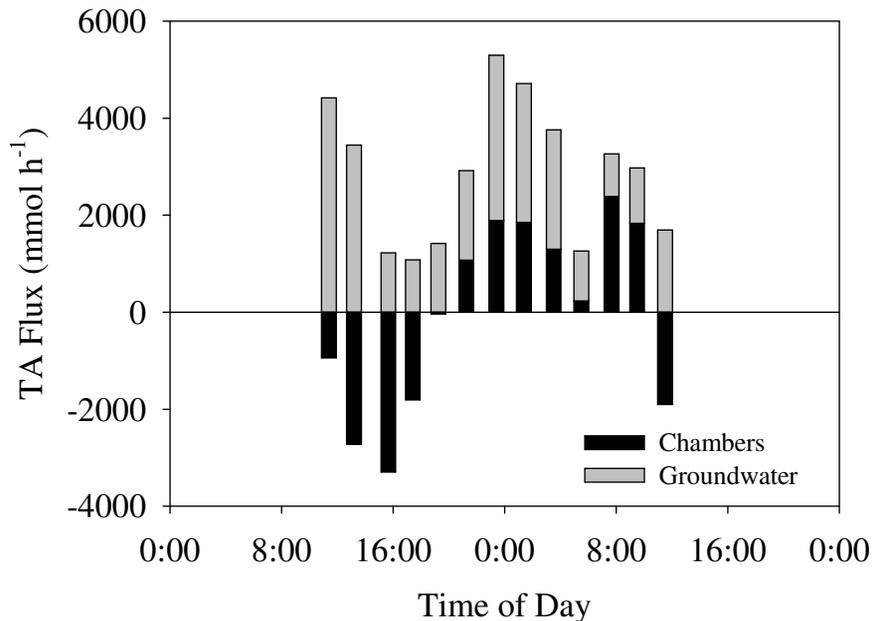
Fig. 12. Hourly flux rates of TA from advective sediments and SGD over a 750 m transect from the study site to reef crest. 100 % cover was assumed for advective sediments and SGD was estimated as mixing 50 m offshore.